Electronic Supplementary Material (ESI) for Physical Chemistry Chemical Physics

Supporting Information

Exploring Förster Electronic Energy Transfer in a Decoupled Anthracenyl-based Borondipyrromethene (Bodipy) Dyad

Dan Bai, Andrew C. Benniston, Jerry Hagon, Helge Lemmetyinen, Nikolai Tkachenko, William Clegg and Ross W. Harrington

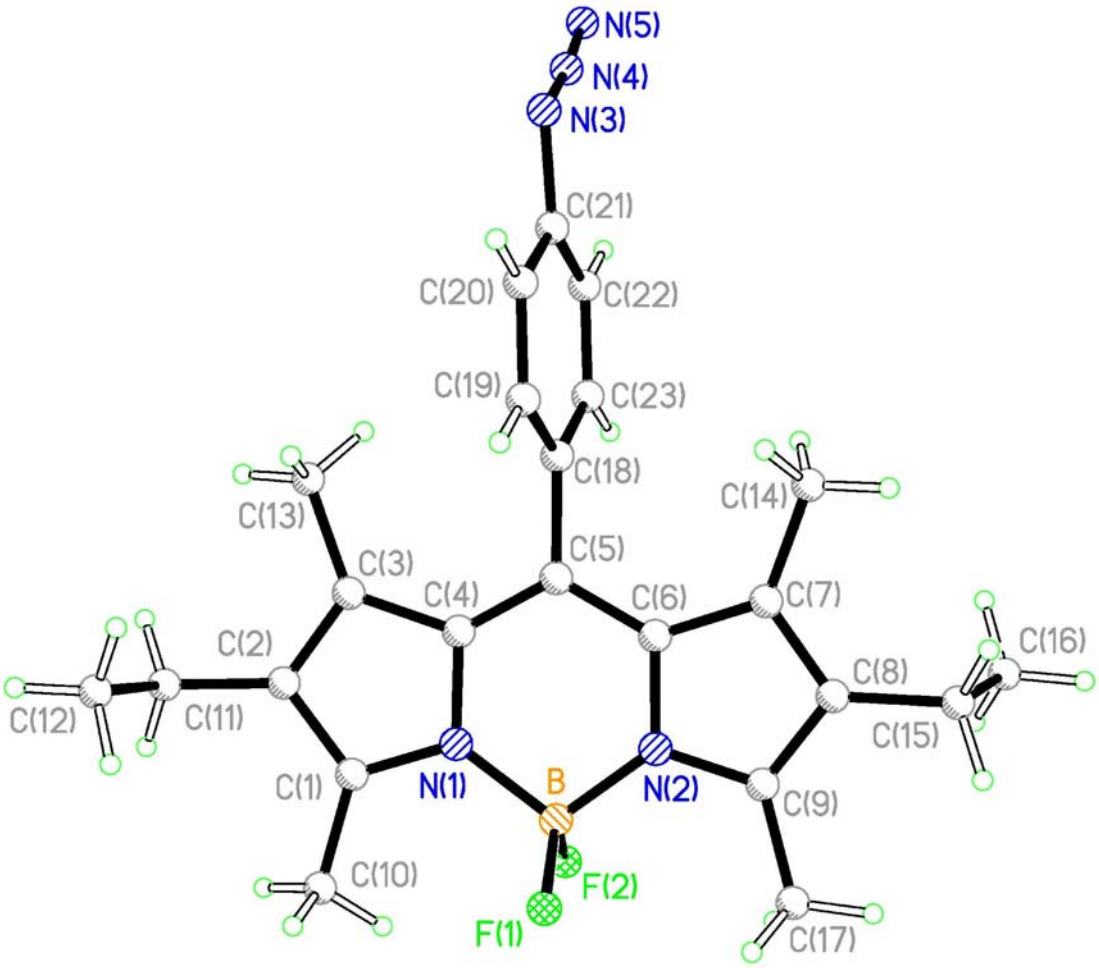

S1. X-ray determined molecular structure for compound **4** showing the atomic labelling.

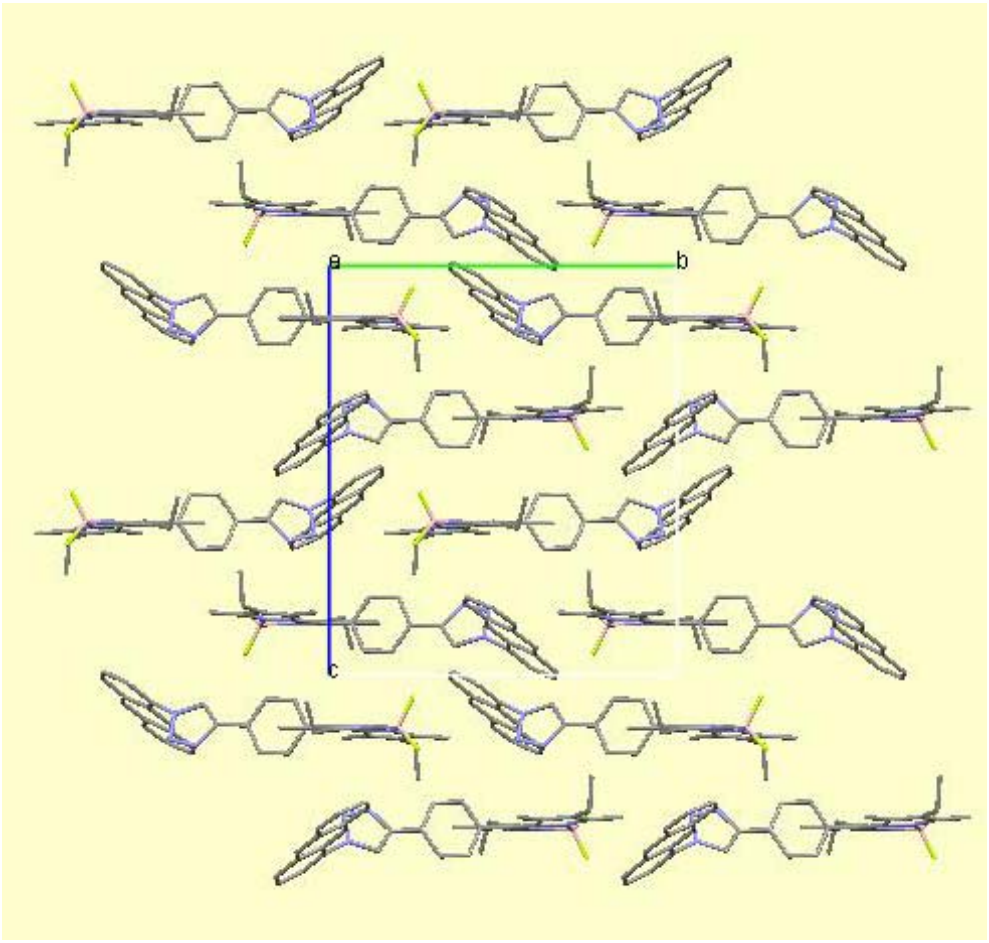

S2. Crystal packing diagram for **ANTBD** in which pairwise stacking of anthracene units and a close approach of triazole CH to an F atom can be seen. H atoms are omitted for clarity; the view is down the *a* axis.

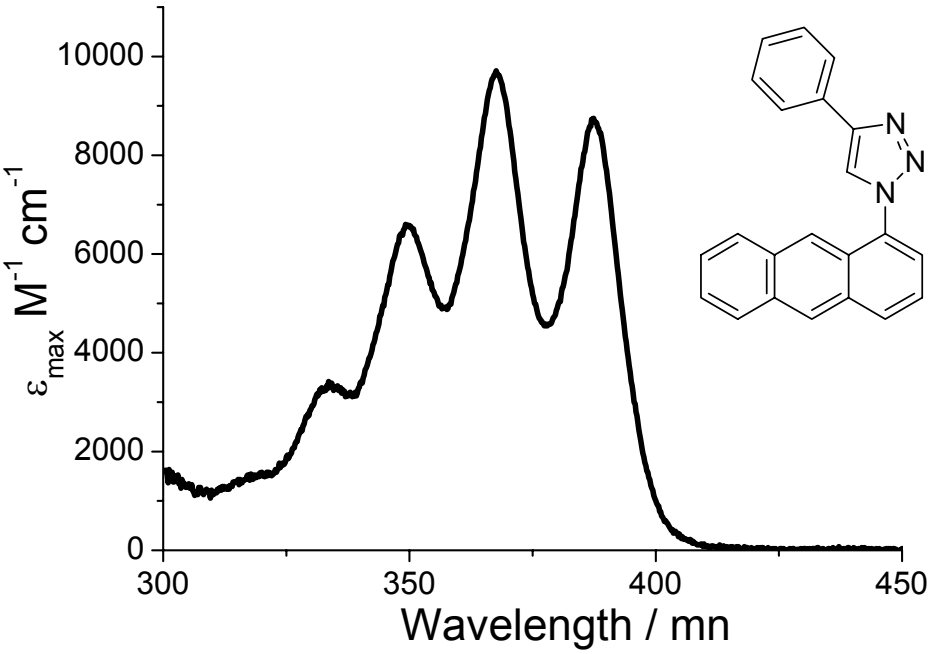

S3. Ambient temperature absorption spectrum for **PHANT** in dry toluene.

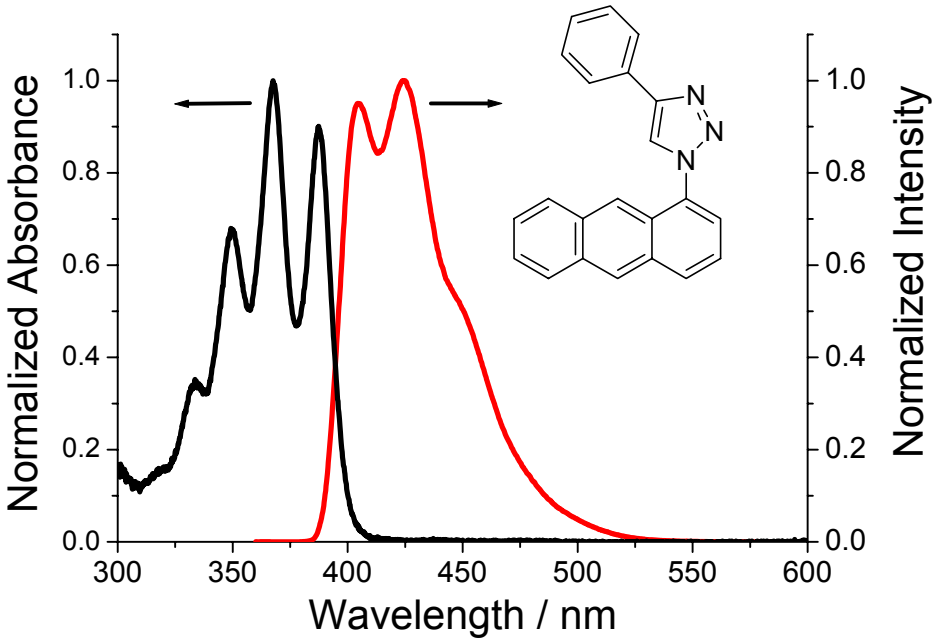

S4. Ambient temperature absorption and fluorescence spectra for **PHANT** in dry toluene.

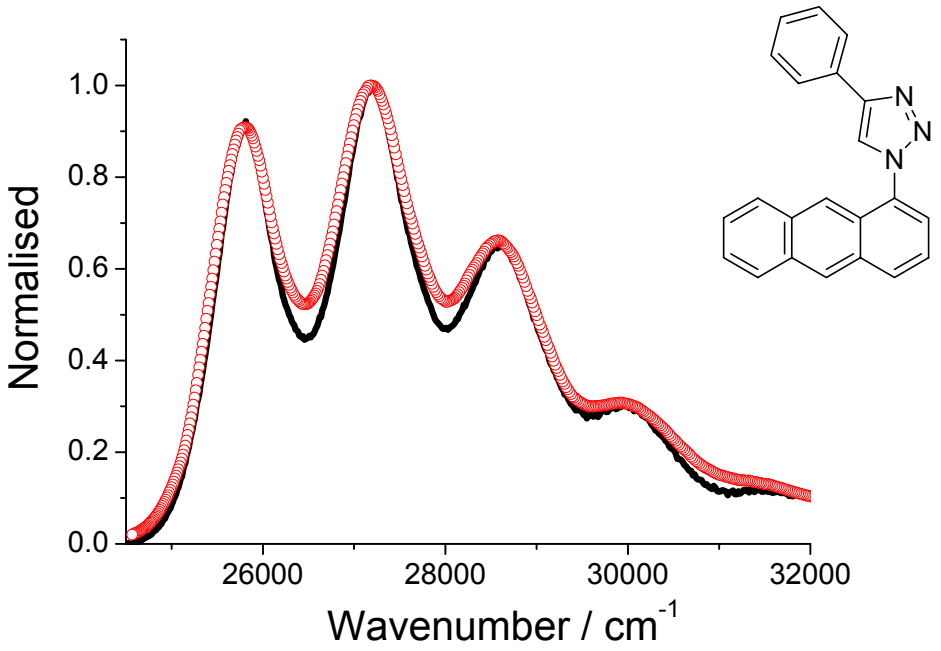

S5. Comparison of the corrected fluorescence excitation spectrum (red) with the absorption spectrum (black) for **PHANT** in dry toluene.

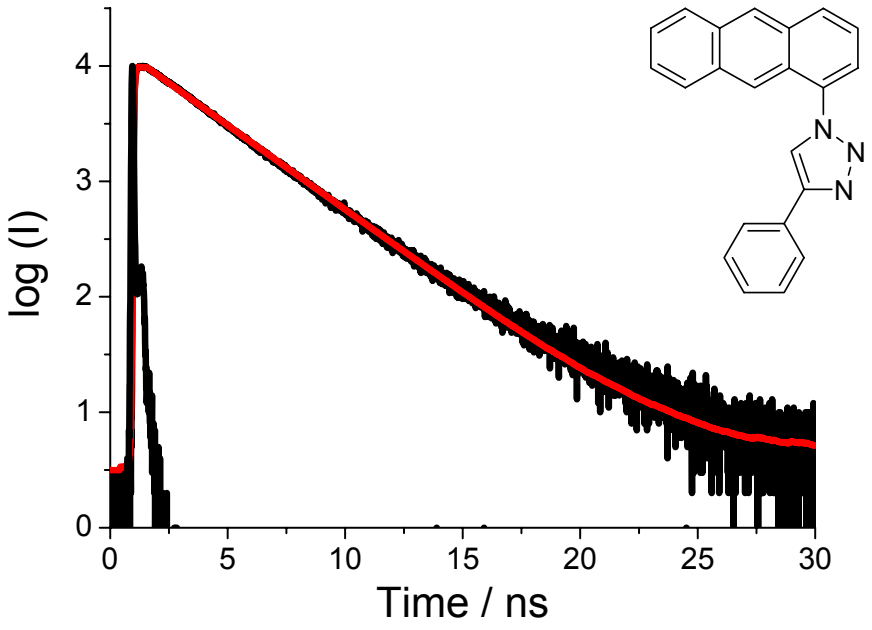

S6. Time-correlated single photon counting fluorescence decay collected for **PHANT** in dry toluene and the least-squares fit to the single exponential (red line). Also shown is the instrument response function.

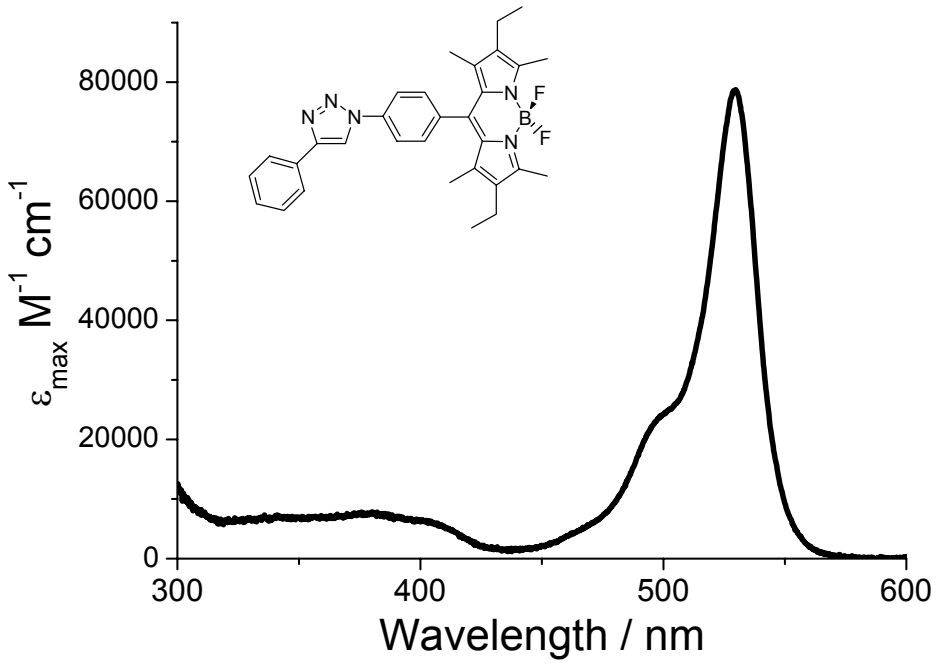

S7. Ambient temperature absorption spectrum for **BD1** in dry toluene.

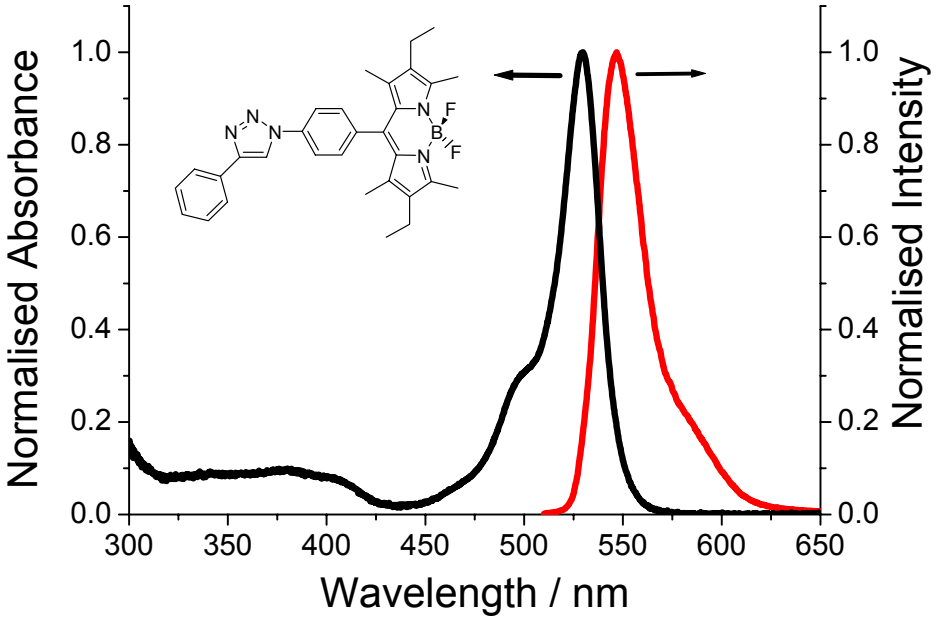

S8. Ambient temperature absorption and fluorescence spectra for **BD1** in dry toluene.

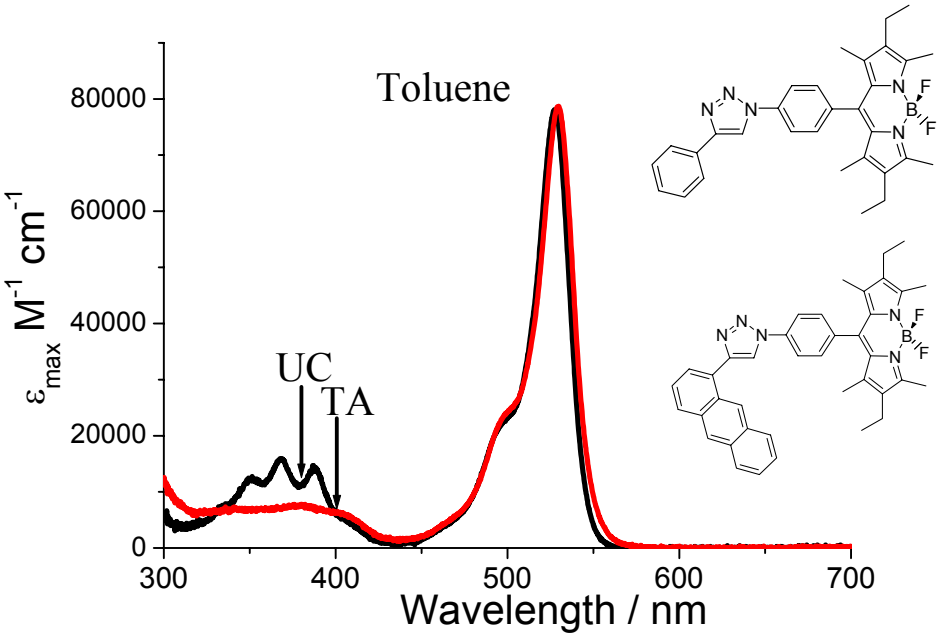

S9. Comparison of the ambient temperature absorption spectra for **BD1** and **ANTBD** in dry toluene. Arrows depict excitation wavelength used for transient absorption (TA) and up-conversion (UC) experiments.

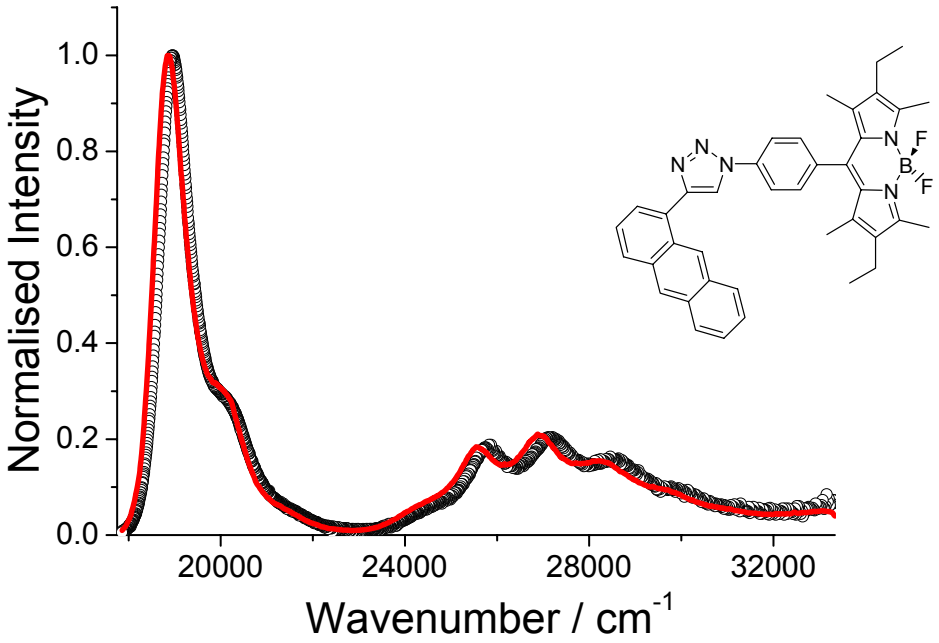

S10. Comparison of the corrected fluorescence excitation spectrum (red) with the absorption spectrum (black) for **BDANT** in dry toluene.

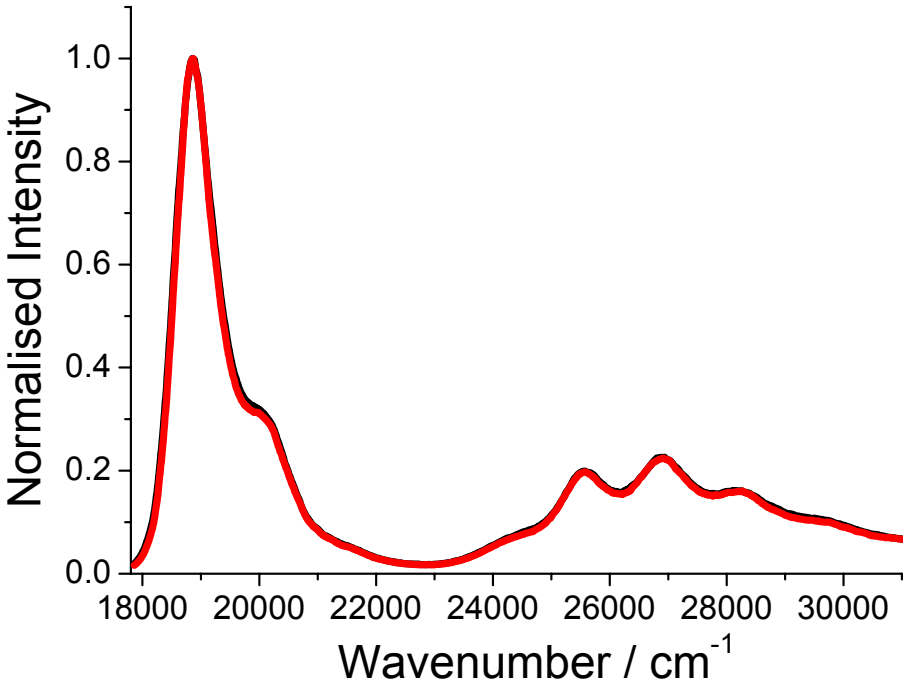

S11. Comparison of the normalised corrected fluorescence excitation spectra for **BDANT** in dry toluene at 293.8K (black) and 279.7 K (red).

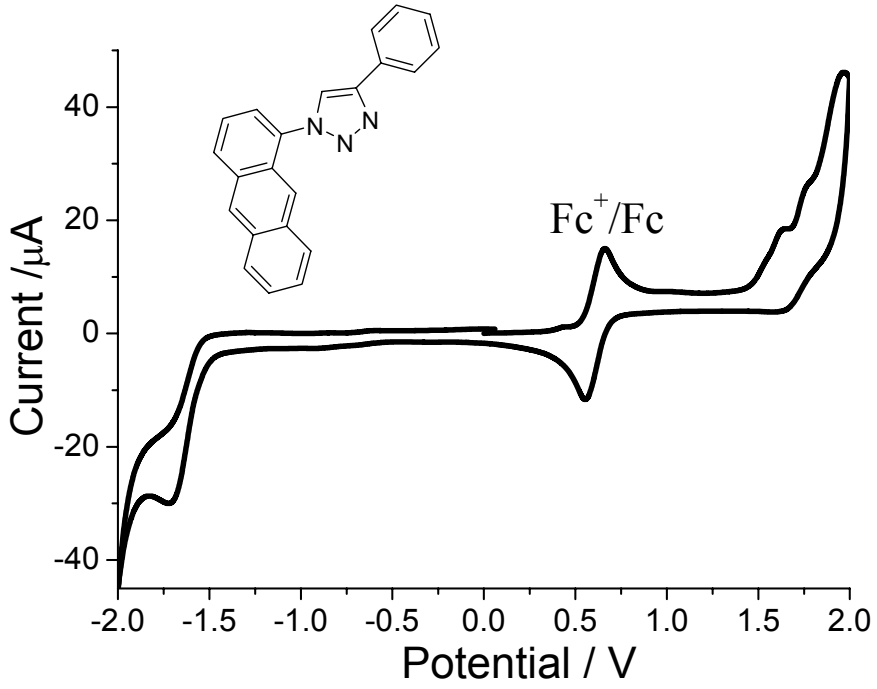

S12. Cyclic voltammogram for **PHANT** in dry DCM (0.2 M TBATFB background electrolyte) at a glassy carbon working electrode and vs Ag wire reference electrode. Scan rate = 50 mV s^{-1}

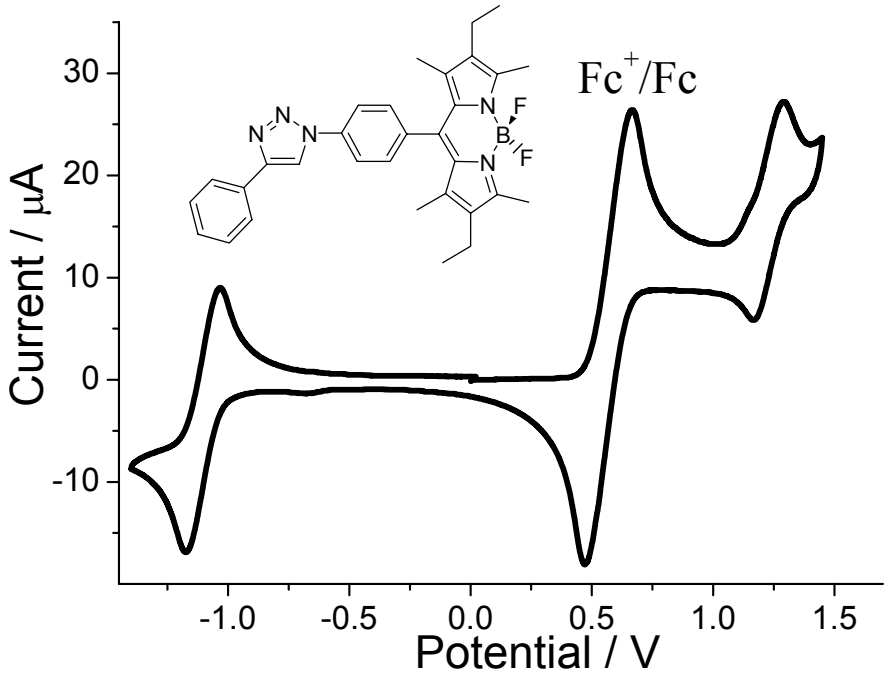

S13. Cyclic voltammogram for **BD1** in dry DCM (0.2 M TBATFB background electrolyte) at a glassy carbon working electrode and vs Ag/AgCl reference electrode. Scan rate = 50 mV s^{-1}

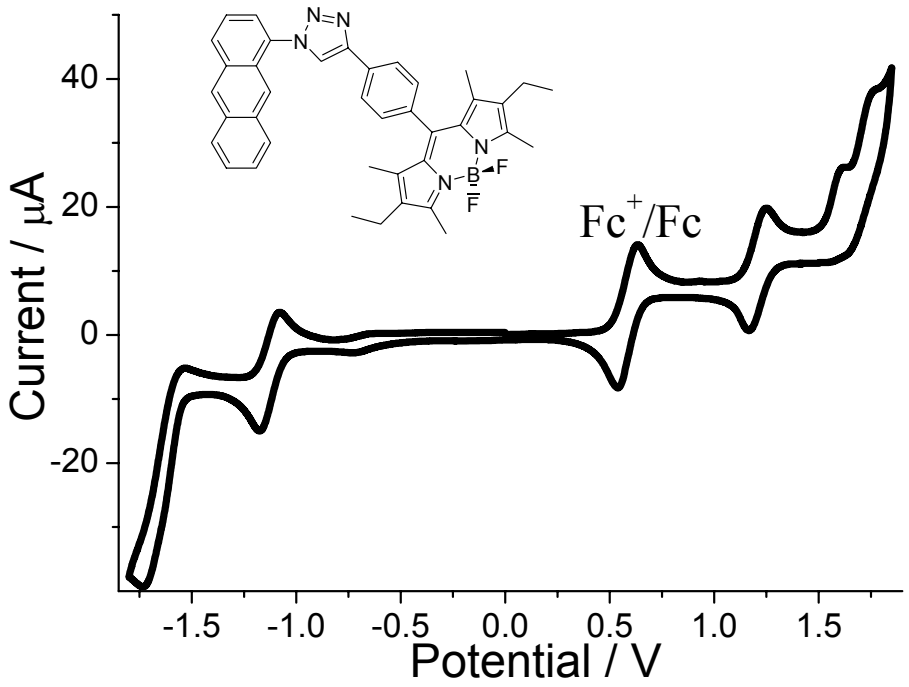

S14. Cyclic voltammogram for **ANTBD** in dry DCM (0.2 M TBATFB background electrolyte) at a glassy carbon working electrode and vs Ag/AgCl reference electrode. Scan rate = 50 mV s^{-1}

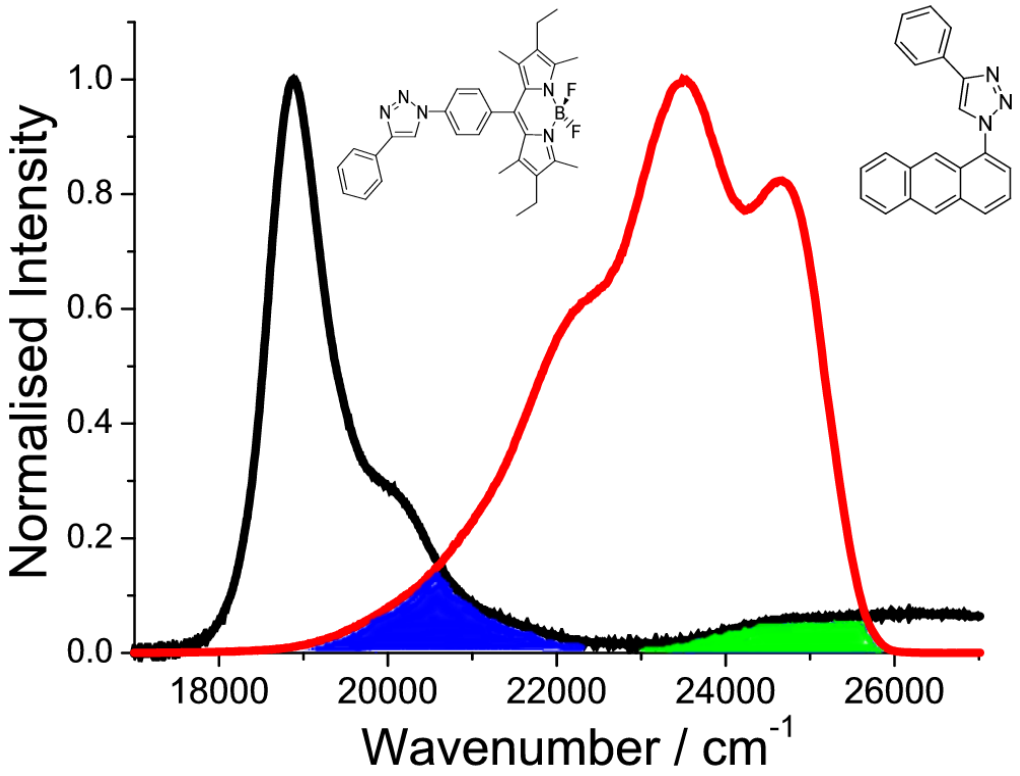

S15. Overlap between emission spectrum for **PHANT** (red) with S_0-S_1 (blue) and S_0-S_2 (green) electronic absorption transitions for **BD1** (black)

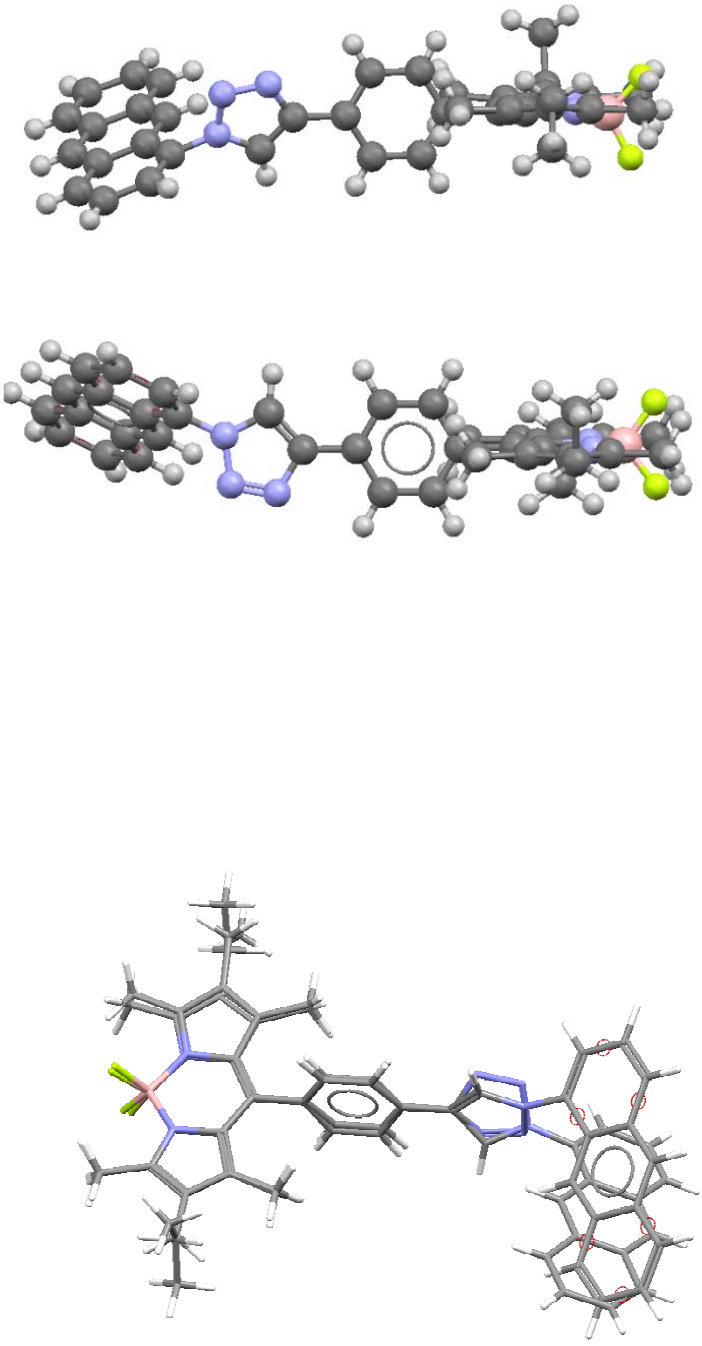

S16. Comparison of the X-ray crystallographic determined structure for **ANTBD** (top) and the computer generated model (middle). The bottom figure shows an overlay of the two structures (N and C atoms of bodipy core)

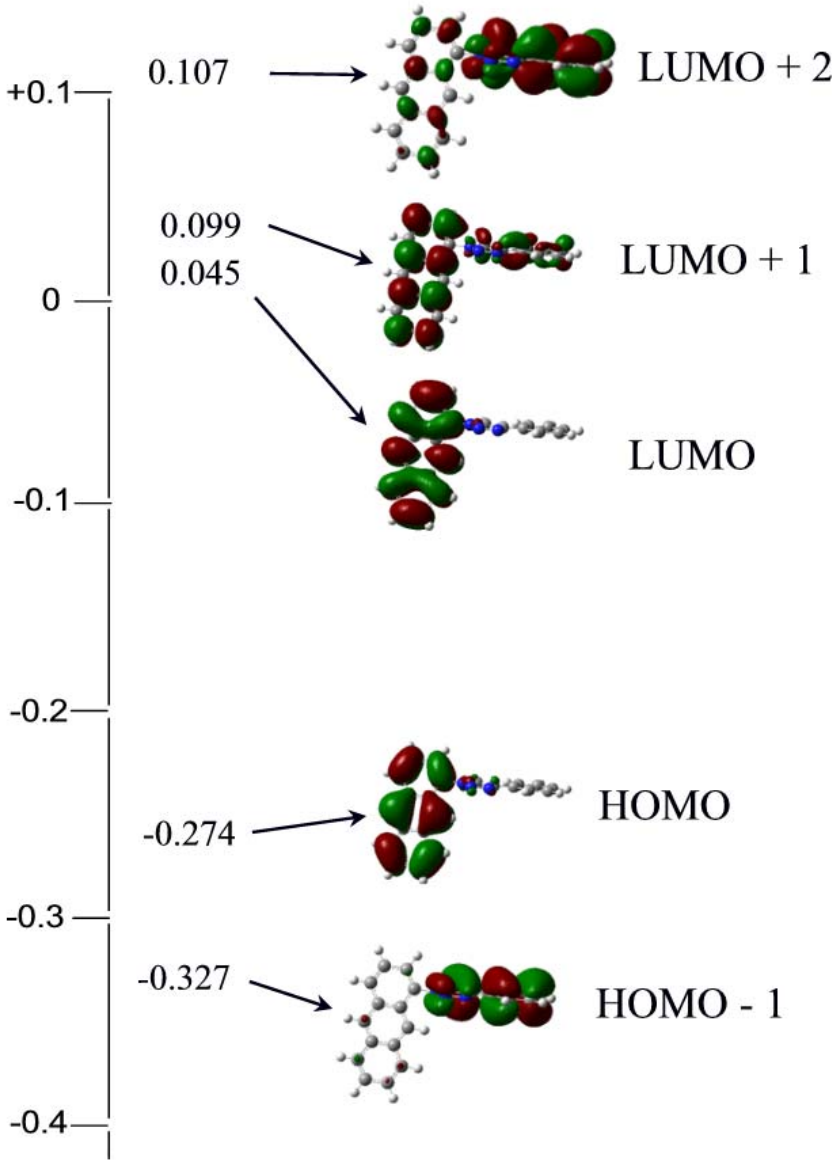

S17. HOMO and LUMO molecular orbitals calculated for **PHANT** using Gaussian-03 at the Hartree-Fock level and using a 6-311G basis set.

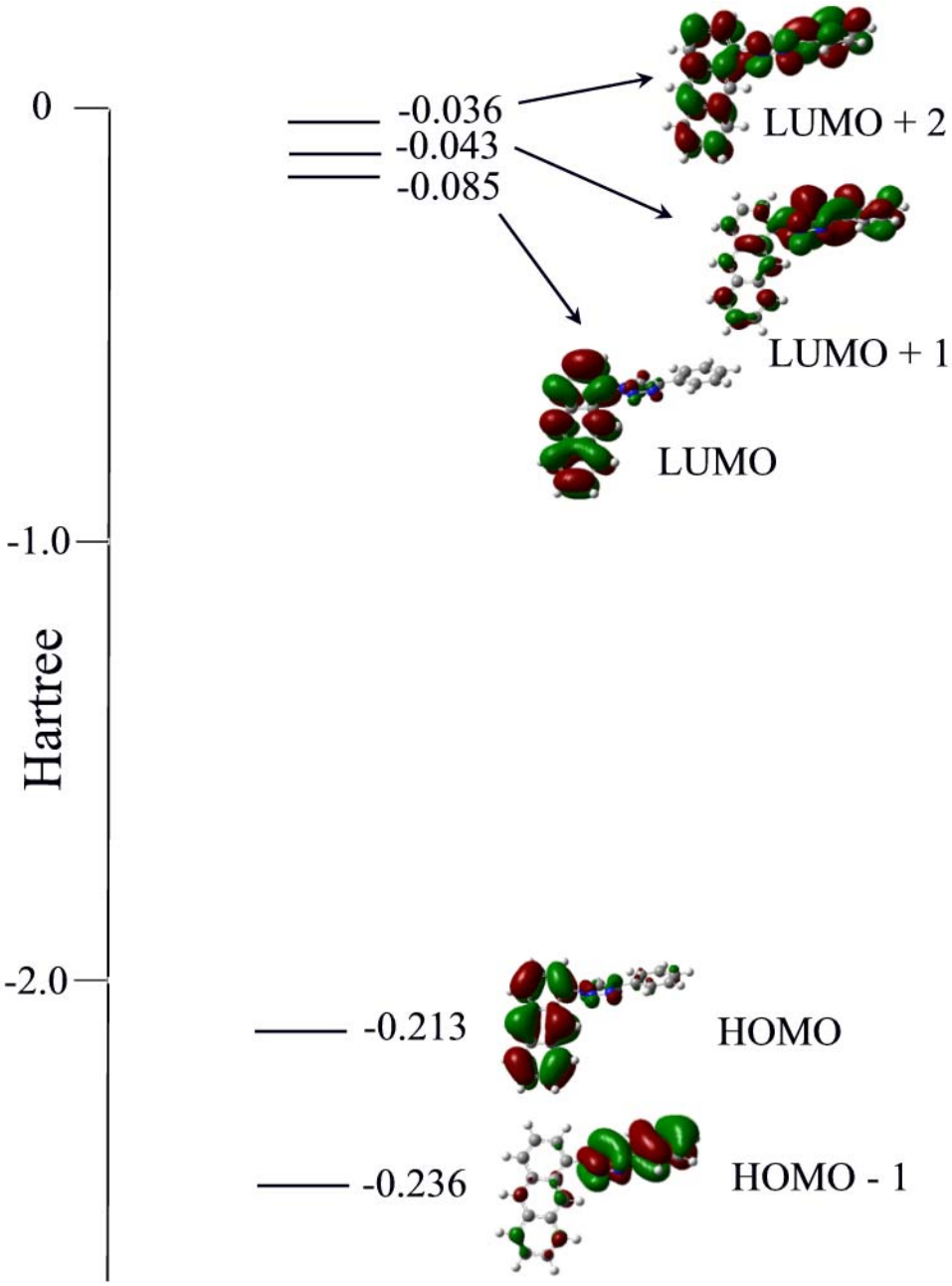

S18. HOMO and LUMO molecular orbitals calculated for **PHANT** using Gaussian-03 and DFT-B3LYP (6-311G basis set).

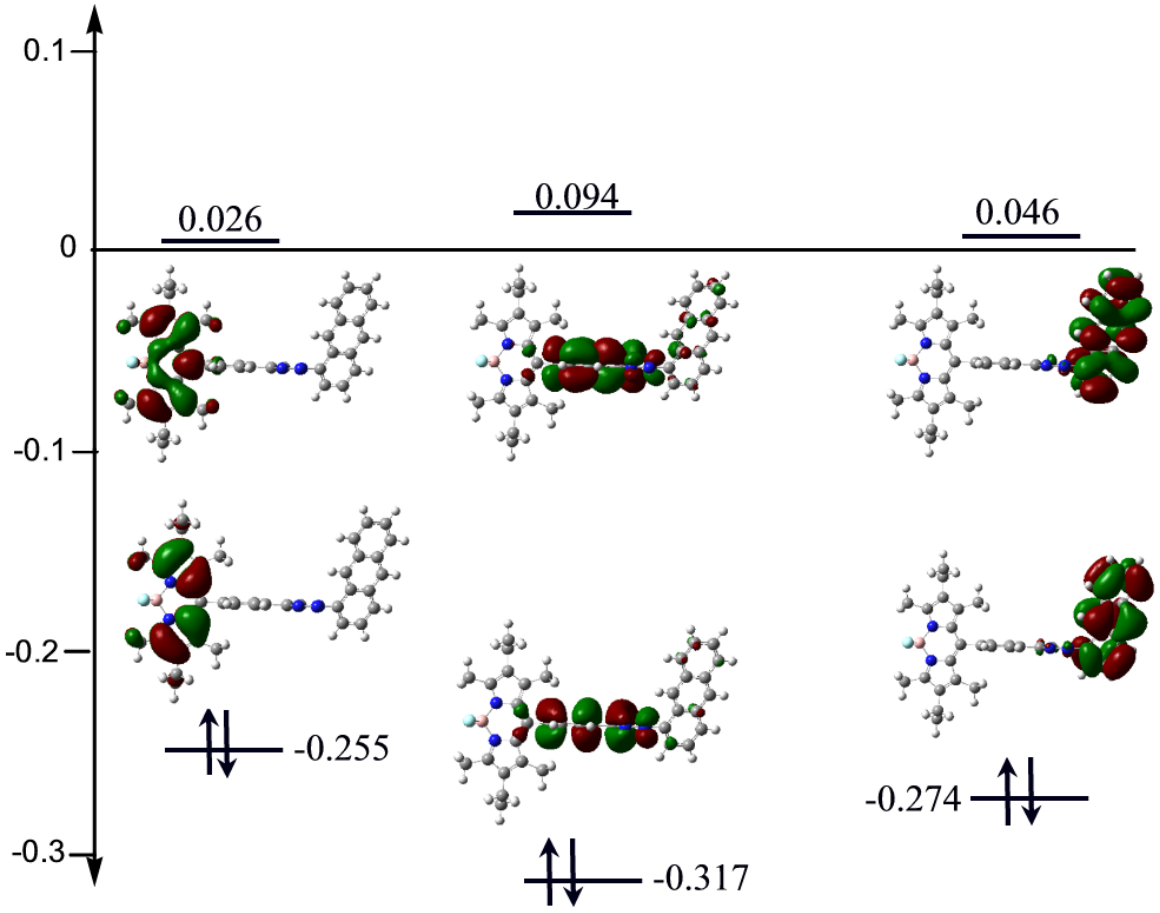

S19. HOMO and LUMO molecular orbitals calculated for ANTBD using Gaussian-03 and Hartree-Fock (6-31G basis set).

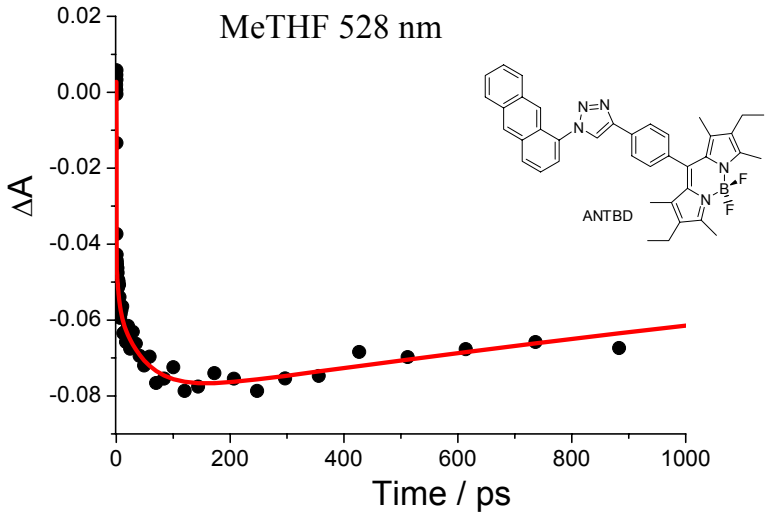

S20. Kinetics recorded at 530 nm (●) and the least-squares fit (red line) to the data points from the transient absorption profiles recorded after excitation of **ANTBD** in Me-THF at 400 nm with a 70 fs laser pulse.

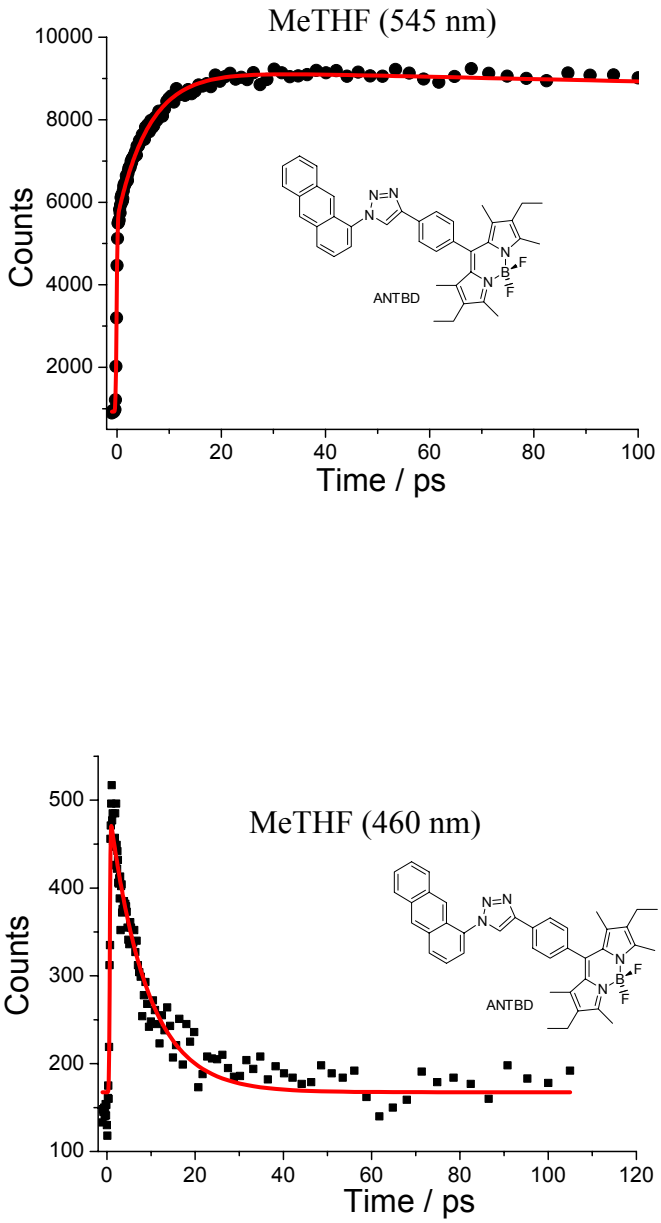

S21. Femtosecond up-conversion profiles recorded at two different wavelengths following excitation of **ANTBD** in MeTHF at 380 nm with a 70 fs laser pulse. Least-squares fit to data points (●) is shown by red line.

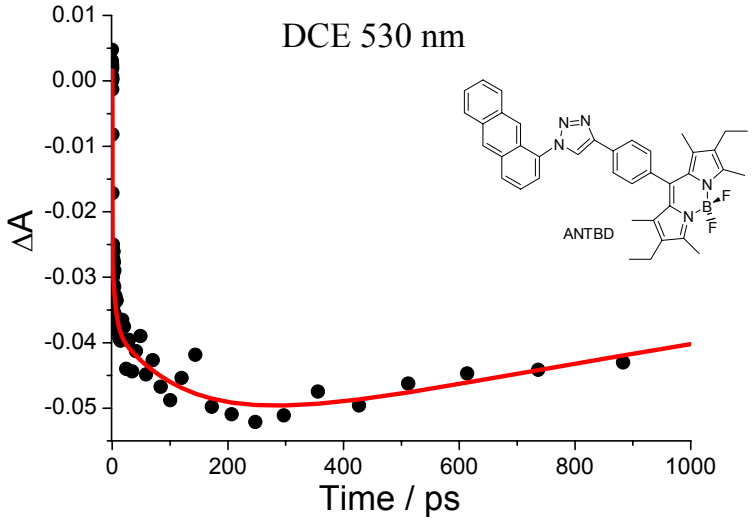

S22. Kinetics recorded at 530 nm (●) and the least-squares fit (red line) to the data points from the transient absorption profiles recorded after excitation of **ANTBD** in DCE at 400 nm with a 70 fs laser pulse.

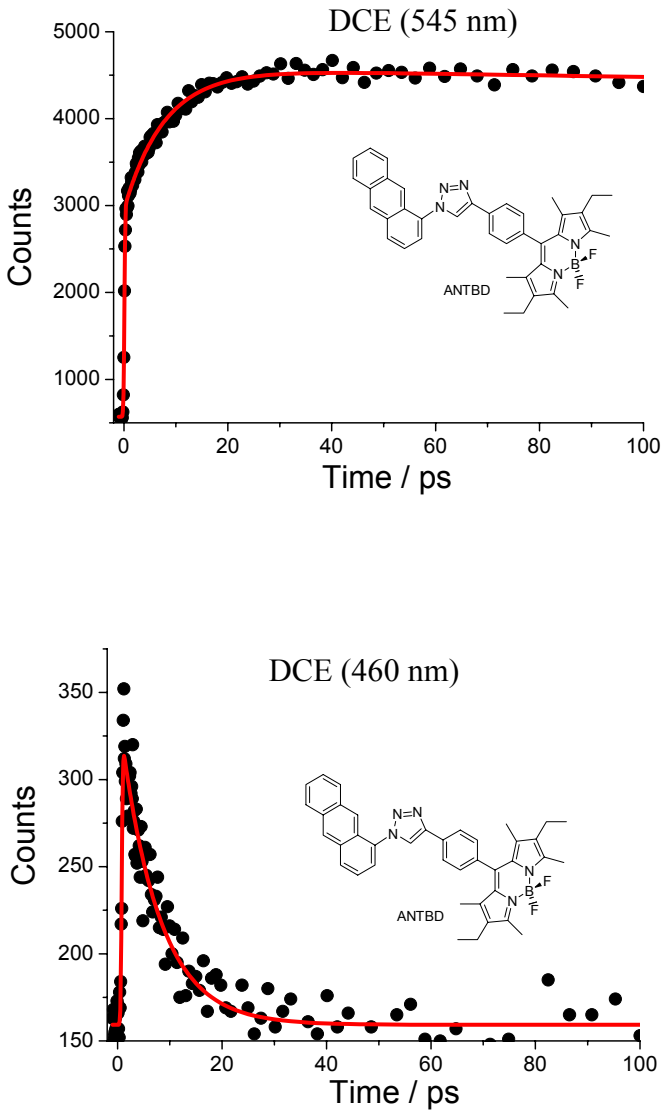

S23. Femtosecond up-conversion profiles recorded at two different wavelengths following excitation of **ANTBD** in DCE at 380 nm with a 70 fs laser pulse. Least-squares fit to data points (●) is shown by red line.

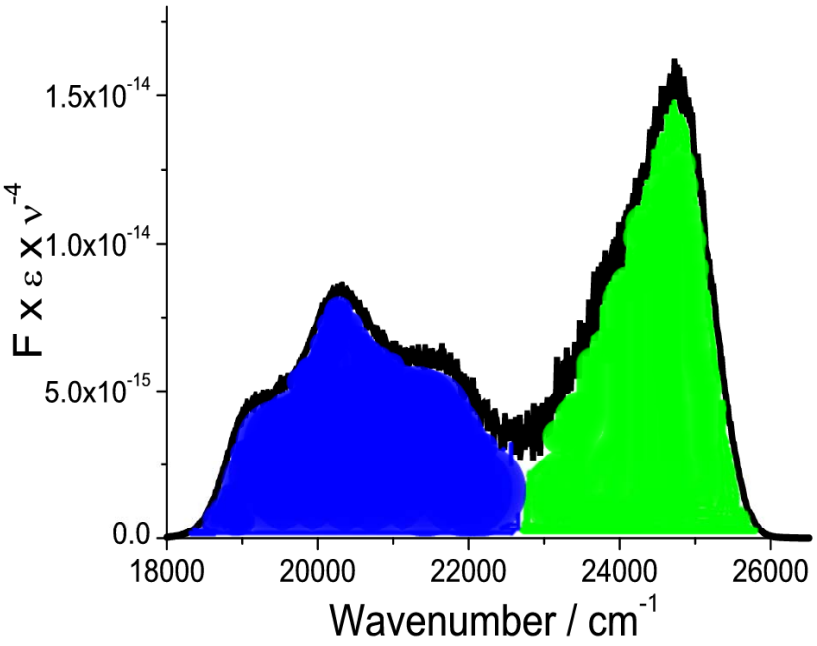

S24. Overlap integral (J_F) calculation result showing the area for the Bodipy-based S_0-S_1 overlap (blue) and S_0-S_2 overlap (green).

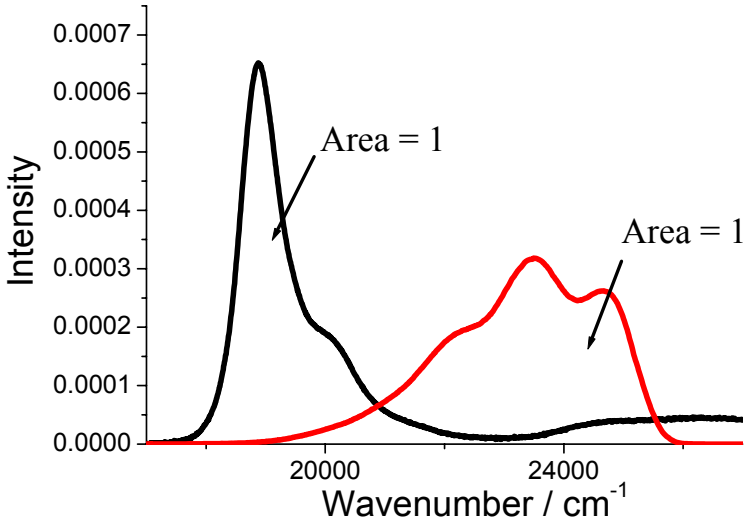

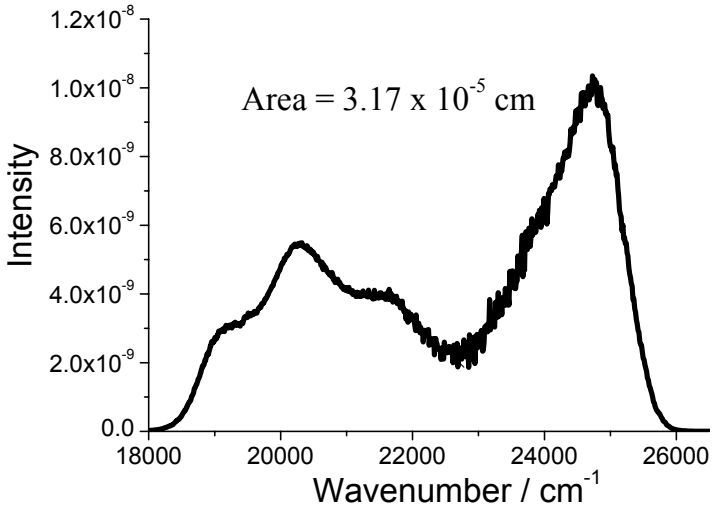

S25. Overlap integral (J_{DA}) calculation result showing the area for the Bodipy-based S_0-S_1 overlap and S_0-S_2 overlap.

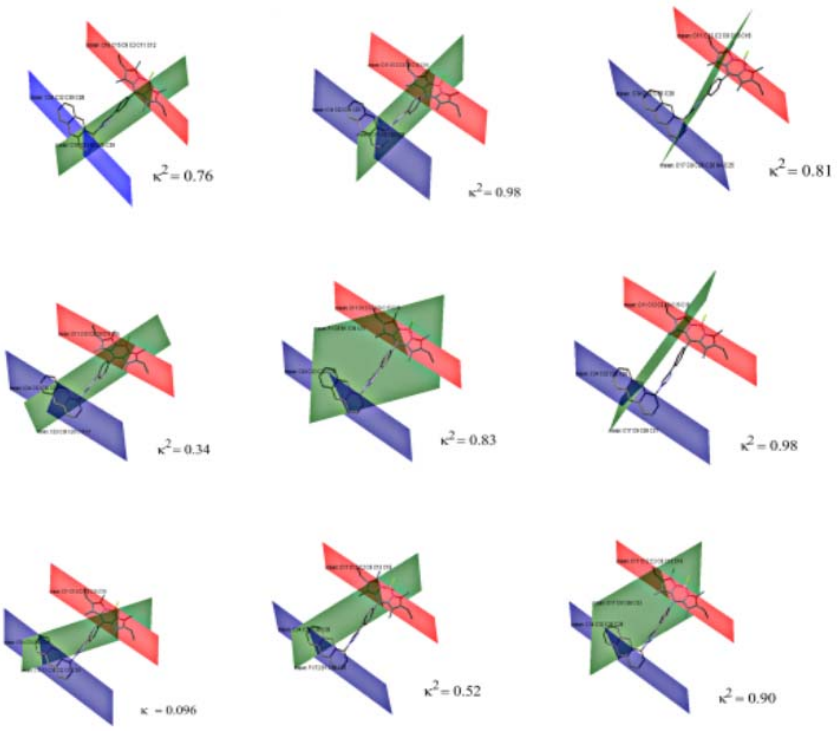

S26. Illustration of generated planes and the corresponding κ^2 values for **ANTBD.**

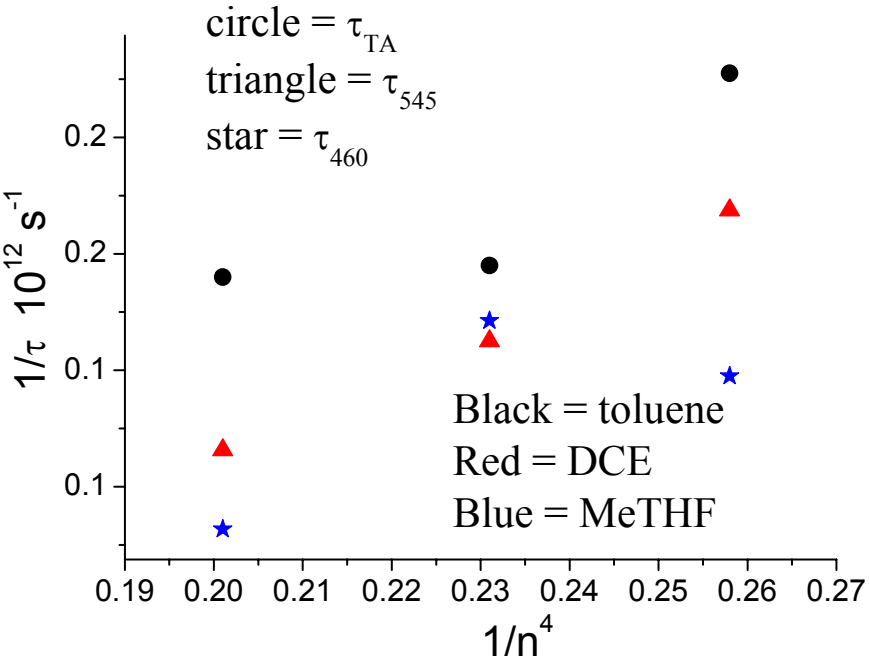

S27. Plots showing the relationships between k_{EET} and $1/n^4$ for **ANTBD.**